Video Article

Polycrystalline Silicon Thin-film Solar cells with Plasmonic-enhanced Light-trapping

Sergey Varlamov[1], Jing Rao[1], Thomas Soderstrom[1]

[1]School of Photovoltaics, University of New South Wales

Correspondence to: Sergey Varlamov at s.varlamov@unsw.edu.au

URL: https://www.jove.com/video/4092
DOI: doi:10.3791/4092

Keywords: Physics, Issue 65, Materials Science, Photovoltaics, Silicon thin-film solar cells, light-trapping, metal nanoparticles, surface plasmons

Date Published: 7/2/2012

Citation: Varlamov, S., Rao, J., Soderstrom, T. Polycrystalline Silicon Thin-film Solar cells with Plasmonic-enhanced Light-trapping. *J. Vis. Exp.* (65), e4092, doi:10.3791/4092 (2012).

Abstract

One of major approaches to cheaper solar cells is reducing the amount of semiconductor material used for their fabrication and making cells thinner. To compensate for lower light absorption such physically thin devices have to incorporate light-trapping which increases their optical thickness. Light scattering by textured surfaces is a common technique but it cannot be universally applied to all solar cell technologies. Some cells, for example those made of evaporated silicon, are planar as produced and they require an alternative light-trapping means suitable for planar devices. Metal nanoparticles formed on planar silicon cell surface and capable of light scattering due to surface plasmon resonance is an effective approach.

The paper presents a fabrication procedure of evaporated polycrystalline silicon solar cells with plasmonic light-trapping and demonstrates how the cell quantum efficiency improves due to presence of metal nanoparticles.

To fabricate the cells a film consisting of alternative boron and phosphorous doped silicon layers is deposited on glass substrate by electron beam evaporation. An Initially amorphous film is crystallised and electronic defects are mitigated by annealing and hydrogen passivation. Metal grid contacts are applied to the layers of opposite polarity to extract electricity generated by the cell. Typically, such a ~2 μm thick cell has a short-circuit current density (*Jsc*) of 14-16 mA/cm^2, which can be increased up to 17-18 mA/cm^2 (~25% higher) after application of a simple diffuse back reflector made of a white paint.

To implement plasmonic light-trapping a silver nanoparticle array is formed on the metallised cell silicon surface. A precursor silver film is deposited on the cell by thermal evaporation and annealed at 23°C to form silver nanoparticles. Nanoparticle size and coverage, which affect plasmonic light-scattering, can be tuned for enhanced cell performance by varying the precursor film thickness and its annealing conditions. An optimised nanoparticle array alone results in cell *Jsc* enhancement of about 28%, similar to the effect of the diffuse reflector. The photocurrent can be further increased by coating the nanoparticles by a low refractive index dielectric, like MgF_2, and applying the diffused reflector. The complete plasmonic cell structure comprises the polycrystalline silicon film, a silver nanoparticle array, a layer of MgF_2, and a diffuse reflector. The *Jsc* for such cell is 21-23 mA/cm^2, up to 45% higher than *Jsc* of the original cell without light-trapping or ~25% higher than *Jsc* for the cell with the diffuse reflector only.

Introduction

Light-trapping in silicon solar cells is commonly achieved via light scattering at textured interfaces. Scattered light travels through a cell at oblique angles for a longer distance and when such angles exceed the critical angle at the cell interfaces the light is permanently trapped in the cell by total internal reflection **(Animation 1: Light-trapping)**. Although this scheme works well for most solar cells, there are developing technologies where ultra-thin Si layers are produced planar (e.g. layer-transfer technologies and epitaxial c-Si layers) [1] and or when such layers are not compatible with textures substrates (e.g. evaporated silicon) [2]. For such originally planar Si layer alternative light trapping approaches, such as diffuse white paint reflector [3], silicon plasma texturing [4] or high refractive index nanoparticle reflector [5] have been suggested.

Metal nanoparticles can effectively scatter incident light into a higher refractive index material, like silicon, due to the surface plasmon resonance effect [6]. They also can be easily formed on the planar silicon cell surface thus offering a light-trapping approach alternative to texturing. For a nanoparticle located at the air-silicon interface the scattered light fraction coupled into silicon exceeds 95% and a large faction of that light is scattered at angles above critical providing nearly ideal light-trapping condition **(Animation 2: Plasmons on NP)**. The resonance can be tuned to the wavelength region, which is most important for a particular cell material and design, by varying the nanoparticle average size, surface coverage and local dielectric environment [6,7]. Theoretical design principles of plasmonic nanoparticle solar cells have been suggested [8]. In practice, Ag nanoparticle array is an ideal light-trapping partner for poly-Si thin-film solar cells because most of these design principle are naturally met. The simplest way of forming nanoparticles by thermal annealing of a thin precursor Ag film results in a random array with a relatively wide size and shape distribution, which is particularly suitable for light-trapping because such an array has a wide resonance peak, covering the wavelength range of 700-900 nm, important for poly-Si solar cell performance. The nanoparticle array can only be located on the rear poly-Si cell surface thus avoiding destructive interference between incident and scattered light which occurs for front-located nanoparticles [9]. Moreover, poly-Si thin-film cells do not requires a passivating layer and the flat base-shaped nanoparticles (that naturally result from thermal annealing of a metal film) can be directly placed on silicon further increases plasmonic scattering efficiency due to surface plasmon-polariton resonance [10].

The cell with the plasmonic nanoparticle array as described above can have a photocurrent about 28% higher than the original cell. However, the array still transmits a significant amount of light which escapes through the rear of the cell and does not contribute into the current. This loss can be mitigated by adding a rear reflector to allow catching transmitted light and re-directing it back to the cell. Providing sufficient distance between the reflector and the nanoparticles (a few hundred nanometers) the reflected light will then experience one more plasmonic scattering event while passing through the nanoparticle array on re-entering the cell and the reflector itself can be made diffuse - both effects further facilitating light scattering and hence light-trapping. Importantly, the Ag nanoparticles have to be encapsulated with an inert and low refractive index dielectric, like MgF_2 or SiO_2, from the rear reflector to avoid mechanical and chemical damage [7]. Low refractive index for this cladding layer is required to maintain a high coupling fraction into silicon and larger scattering angles, which are ensured by the high optical contrast between the media on both sides of the nanoparticle, silicon and dielectric [6]. The photocurrent of the plasmonic cell with the diffuse rear reflector can be up to 45% higher than the current of the original cell or up to 25% higher than the current of an equivalent cell with the diffuse reflector only.

Video Link

The video component of this article can be found at https://www.jove.com/video/4092/

Protocol

1. Fabrication of polycrystalline silicon solar cells (Animation 3)

1. Silicon film deposition
   a. Prepare the e-beam evaporation tool by baking it out at ~100 °C overnight to reach the base pressure of <3E-8 Torr. Preset the sample heater to the 150 °C standby temperature.
   b. Use a substrate made of 5x5 cm^2 (or 10 x10 cm^2) substrate borosilicate glass (Schott Borofloat33), 1.1 or 3.3 mm thick, coated with ~80 nm of silicon nitride (prepared by PECVD from N_2 and SiH_4 mixture).
   c. Blow the surface of the substrate with dry nitrogen to remove dust and place it into a sample holder. Vent the load lock, load the sample, pump the load-lock down to the pressure <1E5 Torr, and transfer the sample to the main chamber. Start the heater to the set-point of 250 °C. Pump for about 20 min when the pressure reaches 8E-8 Torr or lower.
   d. Check that the dopant source and the silicon source shutters are closed. Preset dopant source temperatures to standby temperatures, i.e. the phosphorous source temperature at 700 °C and boron source temperature at 1250 °C. Start e-gun and melt silicon in a crucible by slowly increasing the e-gun current.
   e. When the required current is reached (from previous calibration: this current can vary depending of the e-gun and the Si source conditions) evaporate silicon layers doped with the required concentrations of P and B: 35 nm emitter at 1E20 cm^{-3} of P; 2~3 µm absorber at 5E15 cm^{-3} of B; 100 nm back-surface field (BSF) at 4E19 cm^{-3} of B. The exact dopant concentrations are achieved by matching certain Si deposition rates, as measured by Quartz Crystal Monitor (QCM), with certain dopant source temperatures, using relationships established from SIMS calibration.
   f. After evaporation is done switch the heater off, cool down the sample for ~10 min. Transfer the sample to the load-lock, close the gate-valve, vent the load lock and unload the sample with the silicon film.

2. Silicon crystallisation
   If the sample is 10x10 cm^2, it can be cut into four 5x5 cm^2 cell size pieces prior to crystallisation. Place a deposited silicon film on glass (Si film up) on a holder made of roughened and silicon nitride coated Schott Robax glass (to avoid sticking). Load into a nitrogen purged oven preheated to 200-300 °C. Ramp up the temperature up to 600 °C at 3~5 °C/min and anneal for 30 hr. Turn of the oven heater and let oven cool down naturally to ~200 °C (2~3 hr) before unloading the sample. The sample can have a concave shape due to silicon shrinkage during crystallisation. It will flatten during the following rapid thermal processing.
3. Dopant activation and defect annealing (RTA)
   Place the sample with the crystallised film on a holder made of pyrolytic graphite and load to a rapid thermal processor purged with argon. Ramp the temperature up to 600 °C at 1 °C/s, then up to 1000 °C at 20 °C/s, hold for 1 min then cool down naturally to ~100 °C and unload.
4. Surface oxide removal
   Immediately prior to hydrogenation the surface oxide formed on silicon film during crystallisation and RTA must be removed to ensure that the bare silicon film surface is exposed to hydrogen. Immerse the annealed sample into 5% HF solution until the silicon surface turns hydrophobic (30~100 s). Rinse with deionised water and dry with a nitrogen gun.
5. Defect passivation
   Load the sample into a vacuum chamber equipped with the remote hydrogen plasma source. Pump down to <1E-4 Torr, heat up the sample up to ~620 °C, turn on the argon/hydrogen mixture flow (50:150 sccm), set pressure 50-100 mTorr, start the plasma source at 3.5 kW of the microwave power and continue the process for ~10 min. Turn the heater off while maintaining the plasma for another 10-15 min until the temperature falls down below 350 °C before turning the plasma off and stopping the gas flow. Unload the sample when the temperature is below 200 °C.
6. Cell metallisation
   Cell metallisation is conducted in a series of consecutive photolithographic patterning, Al film deposition and etching steps which are described in details in[11]. The final cell looks like shown in the last slide of ANIMATION 3. A close-up view of the metallised cell is shown in **Fig 1**.
7. Measure EQE of the metallised cell.

2. Fabrication of the Plasmonic Ag Nanoparticle (Animation 4)

1. Blow the metallised cell surface with dry nitrogen to remove dust and load the sample into a thermal evaporator containing a W boat filled with Ag granules (0.3-0.5 g). Pump down the evaporator chamber to the base pressure of 2~3E-5 Torr. Program QCM with parameters for Ag: Density 10.50 and Z ratio 0.529.
2. Ensure that the sample shutter is closed, turn the W boat heater on and increase the current slowly enough to avoid pressure rise above 8E-5 Torr until Ag granules melt (as observed through a view-port). After pressure stabilises set the current to the set point corresponding the Ag deposition rate of 0.1-0.2 Å/s (from calibration) and open the shutter to start the deposition process.
3. Monitor the growing Ag film thickness using QCM and close the shutter when the thickness of 14 nm is reached. Allow the W boat cool down for about 15 min, unload the sample. The film should be annealed to form nanoparticles as soon after deposition as possible to avoid Ag oxidation.
4. A cell with a freshly deposited Ag film is placed into a nitrogen purged oven preheated to 230 0.1-0.2 °C, annealed for 50 min, and then unloaded. Note the change in surface appearance due to nanoparticles. Scanning electron microscopy image of Ag nanoparticles is shown in **Fig. 2**.
5. Measure EQE of the cell with the nanoparticle array.

3. Fabrication of the Rear Reflector

The rear reflector consists of ~300 nm thick MgF_2 (RI 1.38) dielectric cladding with a coat of a commercial white ceiling paint (Dulux).

1. Before fabricating the rear reflector the cell contacts have to be protected by applying a black marker ink on them, which allows exposing the contacts from under the dielectric by a lift-off process.
2. Use nitrogen gun to blow the sample with NP array and painted contacts to remove dust. Use modest nitrogen pressure and exercise care not to blow the nanoparticles away. Place the sample into the thermal evaporator containing a W boat filled with MgF_2 pieces. Pump down the evaporator to pressure of 2~3E-5 Torr. Set QCM parameters for MgF_2: Density 3.05 and Z ratio 0.637.
3. Ensure that the sample shutter is closed, turn on the boat heater and slowly increase the current to avoid excessive pressure rise until MgF_2 melts as seen through a view-port. After the pressure stabilises set the current to the set point corresponding the MgF_2 deposition rate of 0.3 nm/s and open the sample shutter.
4. Monitor the deposited thickness using QCM and close the shutter when 300 nm is reached.
5. Turn off the heater. Allow the W boat to cool down for about 15 min, unload the sample. Note the change in the cell appearance with the MgF_2 cladding.
6. To remove the ink mask from the cell contacts immerse the cell with the dielectric cladding into acetone. Wait until the dielectric above the ink starts cracking and lifting off. Keep the cell in acetone until all the ink with the dielectric is removed and the metal contacts are fully exposed. Remove the sample from acetone, rinse with fresh acetone and dry with nitrogen gun.
7. Apply a layer of a white paint (Dulux One-Coat ceiling paint) with a fine soft brush on the whole cell surface carefully avoiding the metal contacts. The paint layer has to be thick enough to be completely opaque (~>0.5 mm), so that no light can be seen when looking through the painted cell at the bright light source. Let paint dry for a day.
8. Measure EQE of the cell with the white paint rear reflector.

4. Representative Results

The solar cell short-circuit current is calculated by integrating the EQE curve over the standard global solar spectrum (air mass 1.5). Both the cell current and its enhancement due to light-trapping depend on the cell absorber layer thickness: the current itself is higher for thicker cells but the current enhancement is higher for thinner devices, see **Table 1** for the respective data and **Animation 5** for EQE curves. The original 2 μm thick cells, without light-trapping, have *Jsc* measured at step 1.7.) of ~15 mA/cm^2. After fabrication of a nanoparticle array, *Jsc* increases up to about 20 mA/cm^2, which is 32% enhancement. It is slightly better than the enhancement effect of 25-30% by the rear diffuse reflector only. After adding the rear diffuse reflector on the MgF_2 cladding to the cell with the plasmonic nanoparticle array, the *Jsc* is increased further to 22.3 mA/cm^2, or about 45% enhancement. Note that for the 3 μm thick cell all currents are higher, up to 25.7 mA/cm^2 while the relative enhancement is slightly lower, 42%: light-trapping has a relatively larger effect in thinner devices.

Cell thickness:	**2 μm**		**3 μm**	
	***Jsc*, mA/cm^2**	**+%**	***Jsc*, mA/cm^2**	**+%**
original cell	15.4		18.1	
Rear diffuse reflector (R)	20.1	30.5	21.5	18.8
Nanoparticles (NP)	20.3	31.8	21.9	21.0
NP/MgF_2/R	22.3	45.3	25.7	42.0

Table 1. Plasmonic cell short-circuit current and its enhancement compared to original cell.

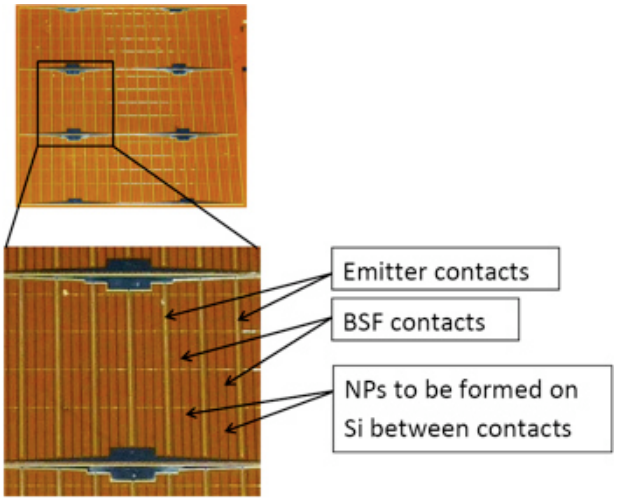

Figure 1. Close-up view of poly-Si thin-film solar cell with metallisation grid.

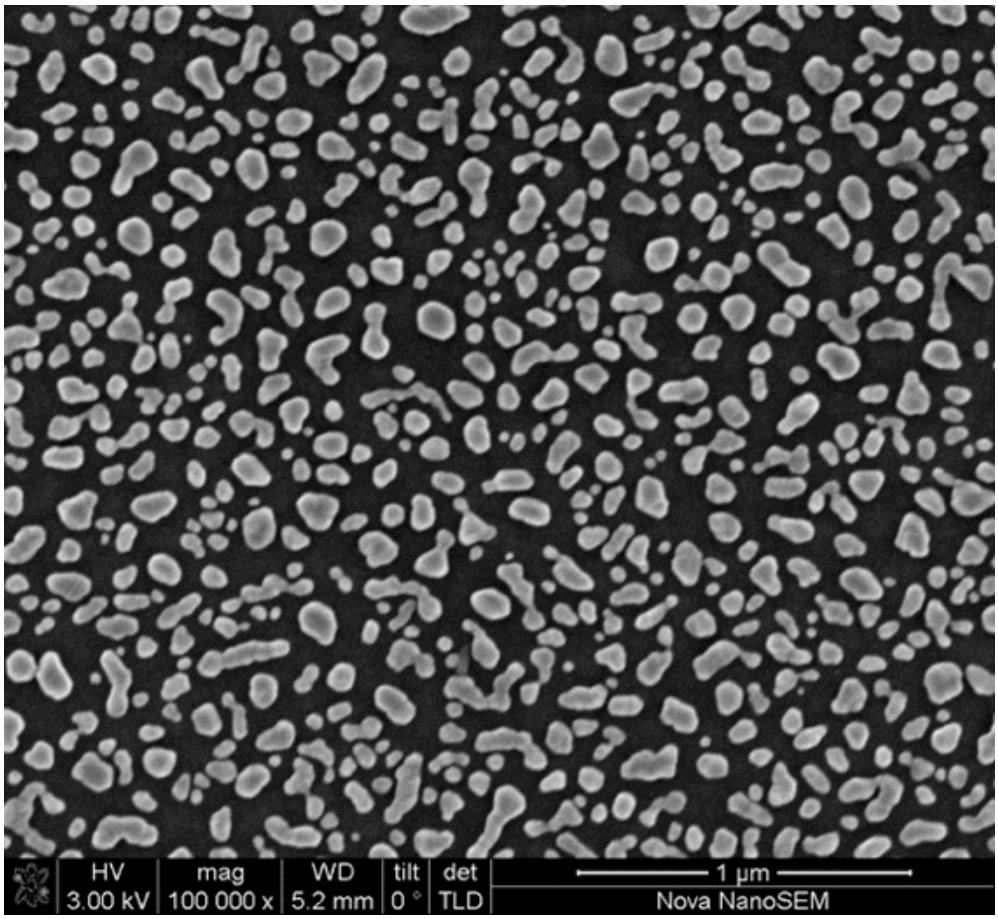

Figure 2. Scanning electron microscopy image of Ag nanoparticles on the silicon surface.

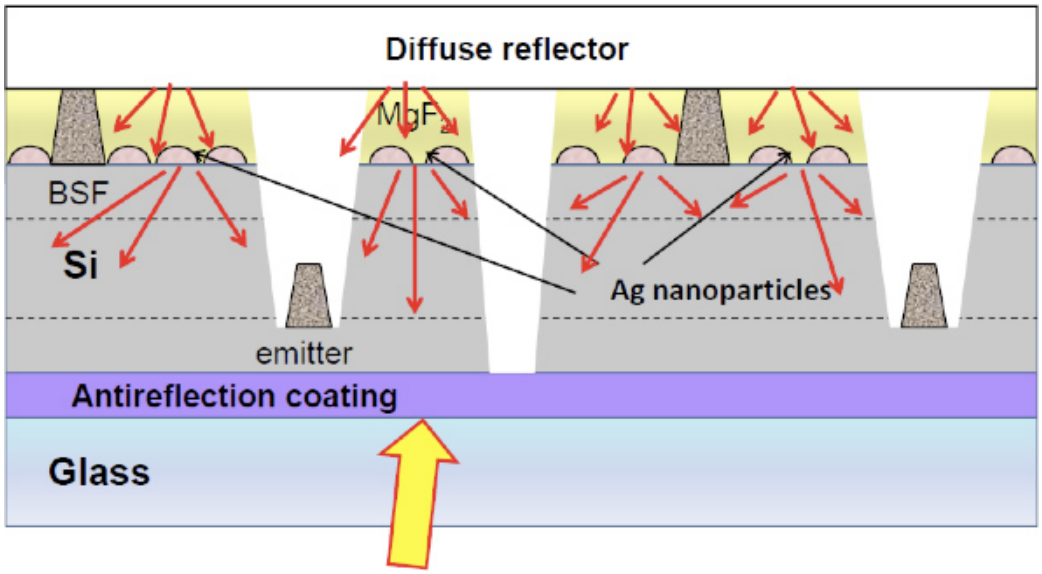

Figure 3. A schematic view of a plasmonic crystalline silicon thin-film solar cell (not to scale).

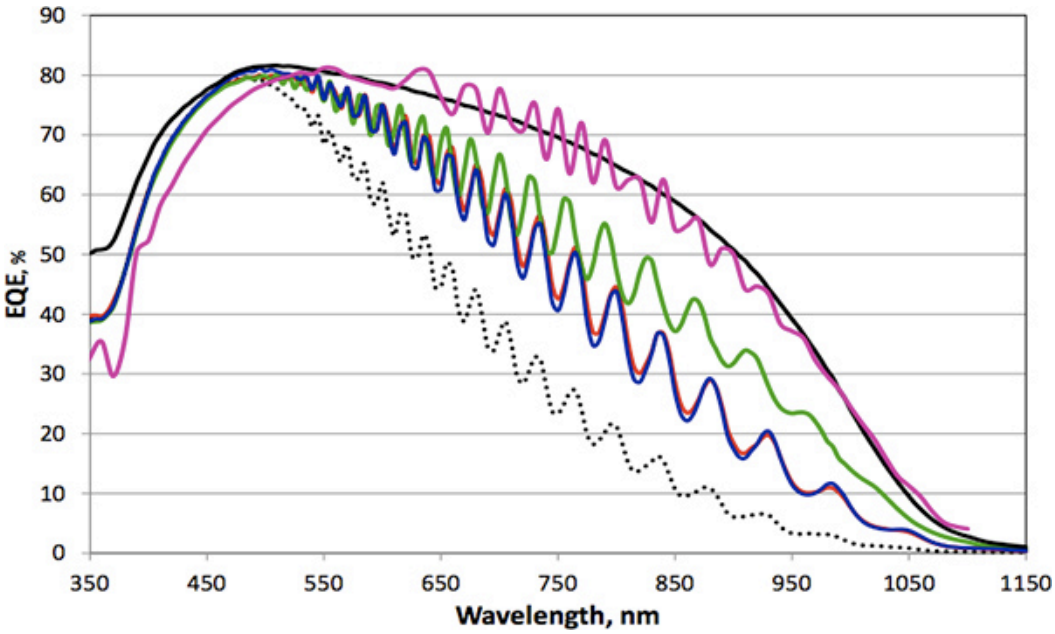

Figure 4. External quantum efficiency and short-circuit current for the polycrystalline silicon thin-film cells with diffuse reflector and plasmonic nanoparticles: dashed-black - original 2 μm thick cell without light-trapping, *Jsc* 15.36 mA/cm^2; blue - cell with diffuse paint reflector, *Jsc* 20.08 mA/cm^2; red - cell with plasmonic Ag nanoparticles, *Jsc* 20.31 mA/cm^2; green - cell with nanoparticles, MgF_2, and diffuse paint reflector, *Jsc* 22.32 mA/cm^2. Purple - 3 μm thick cell (on 3 mm thick glass) with nanoparticles, MgF_2, and diffuse reflector, *Jsc* 25.7 mA/cm^2 (note lower blue response due to unintentional differences in the AR layers and the emitter thickness). Solid black - 2 μm thick textured cell prepared by plasma enhanced chemical vapor deposition (on 3 mm thick glass), *Jsc* 26.4 mA/cm^2, shown for comparison.

Animation 1. Click here to view Animation.

Animation 2. Click here to view Animation.

Animation 3. Click here to view Animation.

Animation 4. Click here to view Animation.

Animation 5. Click here to view Animation.

Discussion

Evaporated polycrystalline silicon solar cells and the light-scattering plasmonic nanoparticles are ideal partners for light-trapping. Such cells are planar, hence they cannot rely on light-scattering from textured surfaces, nor can plasmonic nanoparticles be easily formed on textured

surfaces. The cells have only one, rear surface with directly exposed silicon, which also happens to be the best nanoparticle location for most effective plasmonic light-scattering. Moreover, the easiest method for nanoparticle formation by thermal annealing is also the most suitable for light-trapping because it results in a random nanoparticle array with a broad resonance peak between 700 and 1000 nm, most important for light-trapping in crystalline silicon thin-film cells. As long as functional cells are made, fabrication of the plasmonic reflector is relatively simple and straightforward as described in previous sections. A possible complication is related to fact that the nanoparticles are formed not only on the silicon cell surface but over the metallisation grid pattern as well. It can lead and does sometimes lead to shunting when the nanoparticle relative surface coverage is too large or particularly large nanoparticles are incidentally formed. To avoid cell shunting the coverage should be kept below 50% and the precursor film thickness to be kept below ~20 nm, which is easily achieved considering that the standard process from the 14 nm precursor film, described above, results in 30-35% coverage.

Plasmonic nanoparticle by themselves, with the ~30% *Jsc* enhancement, are about as efficient as, or only slightly better at light-scattering than pigmented paint diffuse reflectors, ~25-30%, which are the simplest to apply. However, while the light-trapping performance of the diffuse paint reflectors cannot be further improved, the plasmonic nanoparticles have an option of being complimented by the diffuse reflectors placed behind them, thus resulting in significantly higher *Jsc* enhancement, up to 45%, than by the nanoparticles alone. This photocurrent enhancement is the highest ever demonstrated for planar crystalline Si thin-film cells, exceeding most recently reported 40% enhancement by a high RI dielectric nanoparticle reflector [5]. Moreover, even higher photocurrent enhancement, exceeding 50%, should be possible with such a high RI nanoparticle diffuse reflector, as described in [5], instead of the commercial white paint.

However, even 45% enhancement is only about half of what is typically achieved in poly-Si thin-film cells fabrication by PECVD on well-textured superstrates, which results in *Jsc* of about 29 mA/cm^2 (~90% enhancement compared to the reference planar cell) [12]. There are two major reasons for much better performance of the cells on textured superstrates. Firstly, the reflection from the textured front cell surface is a lot lower than from the planar surface resulting in more light entering the cell thus generating more current. Antireflection properties of the plasmonic cells with the planar front surface need to be improved to make plasmonic light-trapping more competitive with conventional texturing. Secondly, when two cell interfaces remain planar and parallel, a significant fraction of light is internally and specularly reflected within the cell (~17% at Si/glass or Si/MgF_2 interface) without being scattered by either a diffuse reflector or nanoparticles. This manifests itself in the presence of interference fringes in the cell reflection spectra or in EQE curves of planar cells with diffuse or plasmonic reflectors. Less scattering means less light-trapping, therefore less current enhancement. Textured cells where the light is well-scattered while being reflected at non-parallel interfaces do not have interference fringes as shown in an example EQE curve in **Fig. 2**.

When considering photocurrent enhancement by the plasmonic nanoparticles, as well as by other means applied to the rear side of solar cells, like diffuse reflectors, it is important to remember a trade-off between achieving higher absolute currents or demonstrating higher current enhancement. Thinner devices benefit more from light-trapping, showing higher current enhancement, while the current itself is significantly lower as demonstrated by the results for 2 µm and 3 µm thick cells in Table 1, 22.3 vs. 25.7 mA/cm^2. Similarly, the cells with a poor short wavelength ("blue") response (like those described in [5]) have relatively higher enhancement from light-trapping, which is important to longer wavelength ("red") response, than the cells with a good blue response, but the latter can obviously have a higher absolute current and thus better total performance. As a major goal of photovoltaics is making better performing solar cells, the preference should be given to the light-trapping methods leading to higher absolute currents, not higher current enhancement.

Disclosures

No conflicts of interest declared.

Acknowledgements

This research project is supported by Australian Research Council through the linkage grant with CSG Solar Pty. Ltd. Jing Rao acknowledges her University of NSW Vice-Chancellor Postdoctoral Fellowship. SEM images were taken by Jongsung Park using the equipment provided by the Electron Microscopy Unit of the University of NSW.

References

1. Henley, F.J. Kerf-free wafering. Proc. 35th IEEE Photovoltaic Specialist Conference, Honolulu, USA, 1184-1192 (2010).
2. Kunz, O., Wong, J., Janssens, J., Bauer, J., Breitenstein, O., & Aberle, A. G. Shunting problems due to sub-micron pinholes in evaporated solid-phase crystallised poly-Si thin-film solar cells on glass. *Progress Photovoilt.: Res. Appl.* **17** (1), 35-46 (2009).
3. Kunz, O., Ouyang, Z., *et al.* 5% Efficient evaporated solid-phase crystallised polycrystalline silicon solar cells. *Progress Photovolt.: Res. Appl.* **17** (8), 567-573 (2009).
4. Van Nieuwenhuysen, K., Payo, M. R., *et al.* Epitaxially grown emitters for thin film silicon solar cells result in 16% efficiency. *Thin Solid Films.* **518** (6), S80-S82 (2008).
5. Lee, B.G., Stradin, P., *et al.* Light-trapping by a dielectric nanoparticle back reflector in film silicon solar cells. *Appl. Phys. Lett.* **99**, 064101 (2011).
6. Catchpole, K.R. & Polman, A. Plasmonic solar cells. *Optics Express.* **16** (26), 21793-21800 (2008).
7. Ouyang, Z., Zhao, X., *et al.* Nanoparticle enhanced light-trapping in thin-film silicon solar cells. *Progress Photovolt.: Res. Appl.* **19** (8), 917-926, (2011).
8. Catchpole, K.R. & Polman, A. Design principle for particle plasmon enhanced solar cells. *Appl. Phys. Lett.* **93** (19), 191113 (2008).
9. Beck, F.J., Mokkapati, S., Polman, A., & Catchpole, K.R. Asymmetry in photocurrent enhancement by plasmonic nanoparticle arrays located on the front or on the rear of solar cells. *Appl. Phys. Lett.* **96** (3), 033113 (2008).
10. Beck, F., J., Verhagen, E., *at al.* Resonant SPP modes supported bt discrete metal nanoparticles on high index substrates. *Optics Express.* **19** (2), A146-156 (2010).

11. O. Kunz, Z. Ouyang, *at al.* 5% Efficient evaporated solid-phase crystallised polycrystalline silicon thin-film solar cells. *Progress Photovolt.* **17**, pp. 567-573 (2009).
12. Keevers, M.J., Young, T.L., *et al.* 10% Efficient CSG minimodules, Proc. 22nd European Photovoltaic Solar Energy Conference, Milan, Italy, 1783-1790 (2007).

